J Mater Sci (2011) 46:4710–4714
DOI 10.1007/s10853-011-5381-3

Magnetoelectric properties of $CoFe_2O_4$–$Pb(Zr_{0.52}Ti_{0.48})O_3$ multilayered composite film via sol–gel method

Min Shi · Gui Yang Yu · Hai Lin Su · Ru Zhong Zuo · Yu Dong Xu · Guang Wu · Li Wang

Received: 18 December 2010 / Accepted: 7 February 2011 / Published online: 19 February 2011

Abstract $CoFe_2O_4$–$Pb(Zr_{0.52}Ti_{0.48})O_3$ (CFO–PZT) multilayered composite film was prepared on Pt/Ti/SiO_2/Si substrate via a sol–gel method and spin-coating technique. Results show that PZT and CFO phases exist in the composite film, calcined at 700 °C, besides substrate phase, and no obvious impurity phases can be detected. The composite film exhibits layered structure with obvious boundary between CFO and PZT films. Ferroelectric and ferromagnetic properties were simultaneously observed in the composite film, evidencing the ferroelectric and ferromagnetic properties in the composite film. The composite film exhibits both good magnetic and electric properties, as well as, magnetoelectric (ME) effect. The saturation magnetization value of the composite film is lower than that of the pure CFO film derived by the same processing as a result of the effect of the nonferromagnetic PZT layers. Ferroelectric hysteresis loops reveal that saturated polarization and remanent polarization of the composite film are lower than those of the pure PZT films. The composite film exhibits a very large ME effect, which makes the composite film attractive for technological applications as devices.

M. Shi · G. Y. Yu · H. L. Su (✉) · R. Z. Zuo · Y. D. Xu · G. Wu · L. Wang
School of Materials Science and Engineering, Hefei University of Technology, Hefei 230009, People's Republic of China
e-mail: suhlnju@yahoo.com.cn

M. Shi
e-mail: mrshimin3@hotmail.com

G. Y. Yu
e-mail: yyyuguiyang@126.com

Introduction

Multiferroic materials have drawn many interests due to their potential multi-functional applications on transducers, sensors, and actuators [1, 2]. These materials can not only simultaneously exhibit ferroelectric and magnetic properties, but also a magnetoelectric (ME) effect between the electric and magnetic polarizations [3]. In the recent years, tremendous flurries of research activities have been reported on multiferroic films [4–13]. Many methods have been used for synthesis of composite films, such as pulsed laser deposition [9, 14], electroplating deposition [15], radio frequency sputtering deposition [16, 17], and sol–gel method [18–20]. Among these techniques, sol–gel method is particularly popular due to its advantages such as easy-controlled thickness of the composite film and low cost, a convenient way for studying the ferroelectric and ferromagnetic behaviors and ME effect. Among various materials, $CoFe_2O_4$ (CFO) and $Pb(Zr_{0.52},Ti_{0.48})O_3$ (PZT), as good example of respective ferromagnetic and ferroelectric materials, were intensively investigated for their large magnetostrictive coefficient and piezoelectric coefficient. Alternated CFO–PZT layered films were studied by Nan [10] and depositing sequence of PZT and CFO films was believed to have a noticeable effect on ferroelectric and ferromagnetic properties. Liu [19] prepared a modified CFO–PZT nanocomposite film by polyvinylpyrrolidone-assisted sol–gel method.

However, most efforts have been focused on the double-layered structure, the researches on ME effect of CFO/PZT multilayered composite film are lacking. In this study, CFO–PZT multilayered composite film was prepared by sol–gel processing and spin-coating technique, and the microstructure, multiferroic, and ME properties of the composite film were also dealt with.

Experimental

Preparation

Iron nitrate ($Fe(NO_3)_3 \cdot 9H_2O$), cobalt nitrate ($Co(NO_3)_2 \cdot 6H_2O$), and citric acid ($C_6H_8O_7 \cdot H_2O$) were first dissolved into anhydrous alcohol to form a mixed solution. The molar ratio of Fe^{2+}:Co^{2+}:$C_6H_8O_7$ was 2:1:6. After the solution was stirred for 5 h at 60 °C, CFO precursor solution (0.15 mol/L) was then obtained by adding anhydrous alcohol. Finally, it was continuously stirred for 2 h and placed at room temperature for 24 h to form stable precursor solution of CFO.

Tetrabutyl titanate ($Ti(C_4H_9O)_4$) and zirconium nitrate pentahydrate ($Zr(NO_3)_4 \cdot 5H_2O$) were dissolved into 2-methoxyethanol separately to obtain two kinds of solutions. Lead acetate trihydrate ($Pb(CH_3COO)_2 \cdot 3H_2O$) was dissolved into glacial acetic acid ($CH_3(COOH)_2$) to obtain a solution. The above-mentioned three kinds of solutions were first mixed. Then $Zr(NO_3)_4 \cdot 5H_2O$ solution was added to obtain a homogeneous solution. The molar ratio of Pb^{2+}:Zr^{4+}:Ti^{4+} was 1.1:0.52:0.48 (excessive 10 mol% Pb^{2+} is required to compensate the lead loss during calcination). PZT precursor solution (0.3 mol/L) was obtained by adding 2-methoxyethanol. It was stirred and heated at 60 °C for 24 h to form a stable precursor solution of PZT.

The precursor solution of PZT was spin-coated on the Pt/Ti/SiO_2/Si substrate for two times to form two-layered PZT films at a spinning rate of 3200 rpm for 30 s. The precursor solution of CFO was then spin-coated on the PZT films for four times to form CFO films with four layers. Then CFO and PZT layered films were deposited alternately. The structure of the composite films is 2PZT/4CFO/2PZT/4CFO/2PZT (abbreviated as $P_2C_4P_2C_4P_2$, where P stands for PZT films, C stands for CFO films, and the number in the subscript stands for the layer number of corresponding films). In order to decrease the stress in the composite film, CFO or PZT layered films were calcined at 350 °C for 4 min before depositing another type of layered films. After multi-layered composite film was deposited completely, it was calcined at 700 °C for 10 min.

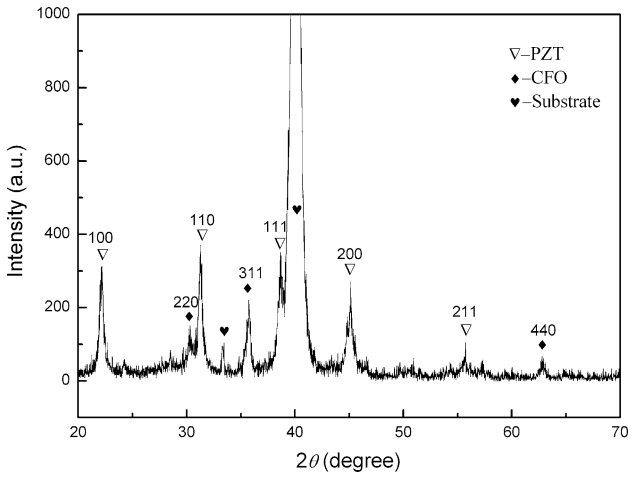

Fig. 1 XRD patterns of the $P_2C_4P_2C_4P_2$ composite film after calcined at 700 °C for 10 min

Characterization

Phase structure of the composite film was evaluated by using an X-ray diffractometer (D/Max-rB, Rigaku, Japan) with CuKα radiation. Cross-section and surface morphologies of films were observed using a field emission scanning electronic microscope (Sirion200, FEI, Netherlands). Magnetic behavior was detected by a vibration sample magnetometer (BHV-55, Riken, Japan). The ferroelectric measurements were carried out on ferroelectric testing unit (TF analyzer 2000, aixACCT, Germany). ME effect of the composite film was measured using a ME measuring device.

Results and discussion

Phase characterization of the composite film

Figure 1 shows the typical X-ray diffraction (XRD) pattern of the composite film, after calcined at 700 °C for 10 min. The diffraction peaks of the perovskite PZT, spinel CFO phases, and substrate phases are observed. In addition, PZT and CFO phases are polycrystalline structures and no obvious impurity phases can be detected. XRD result reveals that there exists no chemical reaction or phase diffusion between the CFO and PZT phases. This will help to improve ME effect of the composite film, as diffusion between the CFO and PZT phases leads to the leakage and low ME effect [10, 21].

Microstructure observation of the composite film

The one-layered CFO film was prepared by spin-coating for one time at a spinning rate of 3200 rpm for 30 s and then calcined at 700 °C for 10 min. Figure 2 shows SEM image of cross section of one-layered CFO film. It can be seen that the thickness of the one-layered CFO film is about 49.0 nm. The interface between CFO film and substrate is difficult to identify. This implies that there exists diffusion between CFO and substrate phases.

The double-layered PZT films were prepared by repeating spin-coating for two times and then calcined at 700 °C for 10 min. Figure 3 shows SEM image of cross section of double-layered PZT films. It can also be seen that the thickness of PZT films is 97.0 nm. The interface

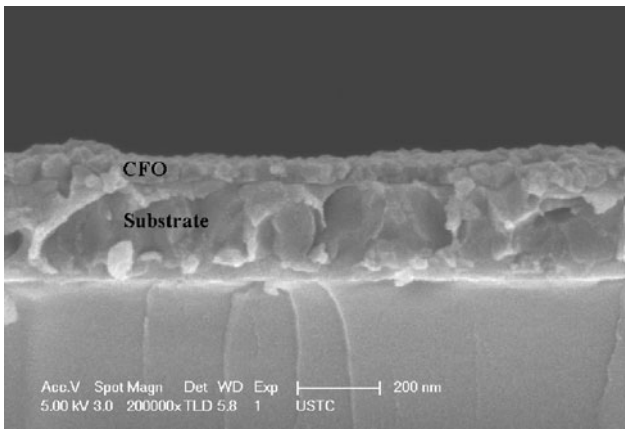

Fig. 2 SEM cross-sectional image of one-layered CFO film after calcined at 700 °C for 10 min

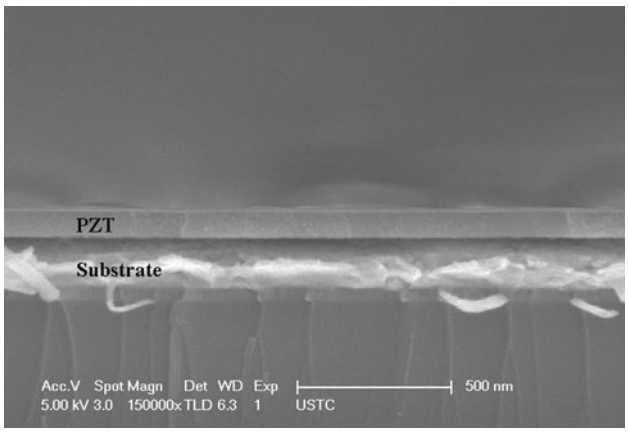

Fig. 3 SEM cross-sectional image of double-layered PZT films after calcined at 700 °C for 10 min

between PZT films and substrate is clear and flat. This implies that there is no obvious diffusion between PZT films and substrate. Therefore, in this article, PZT films were first deposited on substrate, not CFO films were first deposited on substrate, in order to avoid diffusion between phases in the films and substrate phases [22].

Figure 4a shows SEM image of surface of the composite film. It shows that the surface of the composite film possesses a dense and uniform microstructure without obvious micro-cracks, and the average diameter of PZT particles is about 80 nm. The SEM cross-sectional image of the composite film is shown in Fig. 4b. It shows that the composite film exhibits layered structure. In composite films, the thicknesses of four-layered CFO films are near 200 nm and the thicknesses of two-layered PZT films are near 90 nm. The layer boundaries between CFO films and PZT films are clear. It can be deducted that there is no diffusion between CFO phase and PZT phase.

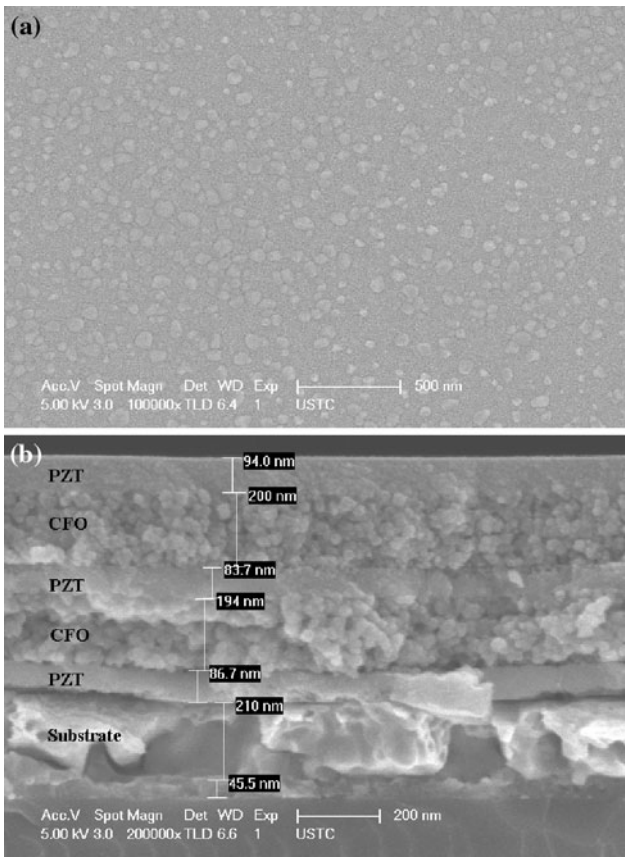

Fig. 4 SEM images of the $P_2C_4P_2C_4P_2$ composite film after calcined at 700 °C for 10 min: **a** surface, **b** cross-section

Ferromagnetic and ferroelectric properties of the composite film

Figure 5 shows typical magnetic hysteresis loops of the composite film and pure CFO film. For the composite film, saturation magnetization (M_s) is 239.5 emu/cm^3, which is much smaller than that of the pure CFO film (i.e., $M_s = 358.45$ emu/cm^3). It is due to the dilute effect of the nonferromagnetic PZT phase. Of interest, the composite film exhibits a greater coercivity (H_c) than that of the pure CFO films (i.e., $H_c = 1262.43$ Oe for the composite film, but 1092.36 Oe for the CFO film, respectively). This may be attributed to the greater stress in the interface between CFO and PZT phases in the composited film, compared with the pure CFO film.

Figure 6 shows polarization–electric field (P–E) hysteresis loops of the composite films and pure PZT films. Both of them show a normal hysteresis behavior. The saturated polarization (P_s) and remanent polarization (P_r) of the composite film are 21.67 and 7.70 μC/cm^2, respectively, which are lower than those of the pure PZT films ($P_s = 42$ μC/cm^2, $P_r = 11$ μC/cm^2). This is due to smaller

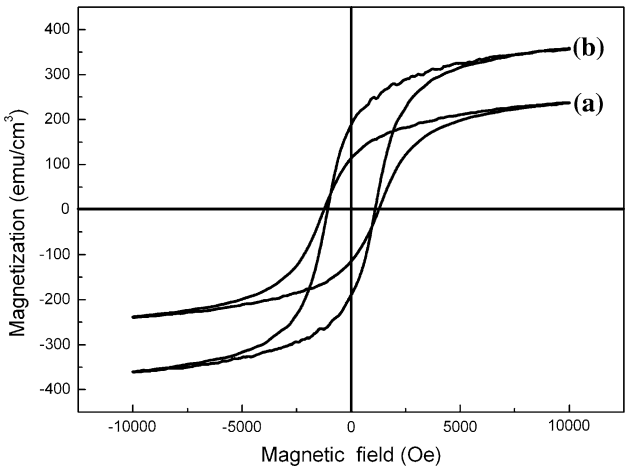

Fig. 5 Magnetic hysteresis loops of the composite film and pure CFO film after calcined at 700 °C for 10 min; *a* $P_2C_4P_2C_4P_2$, *b* pure CFO film

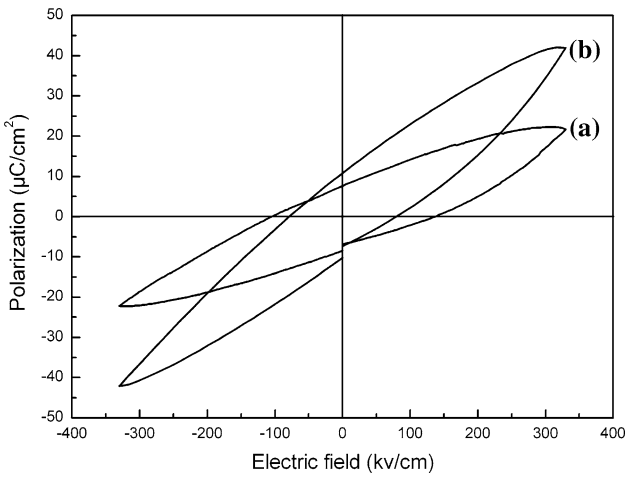

Fig. 6 P–E hysteresis loops of the composite film and pure PZT films after calcined at 700 °C for 10 min: *a* $P_2C_4P_2C_4P_2$, *b* pure PZT films

relative volume fraction of CFO phase in the composite film, compared with the pure CFO film [21, 23].

Magnetoelectric properties of the composite film

The coexistence of the ferromagnetic CFO and ferroelectric PZT phases in the composite film gives rise to ME effect, which is characterized by the ME voltage coefficient α_E. The relationship between α_E and magnetic bias (H_{bias}) for the composite film is shown in Fig. 7. When H_{bias} is zero, the composite film exhibits an initial high α_E value (e.g., 203 mV/cm Oe), greater than that of the bulk ferroelectric–ferromagnetic composite which is nearly close to zero [24, 25]. With the increase of the H_{bias}, the α_E increases quickly and reaches highest value (228 mV/cm Oe) when H_{bias} is near 460 Oe. The maximum α_E value of the

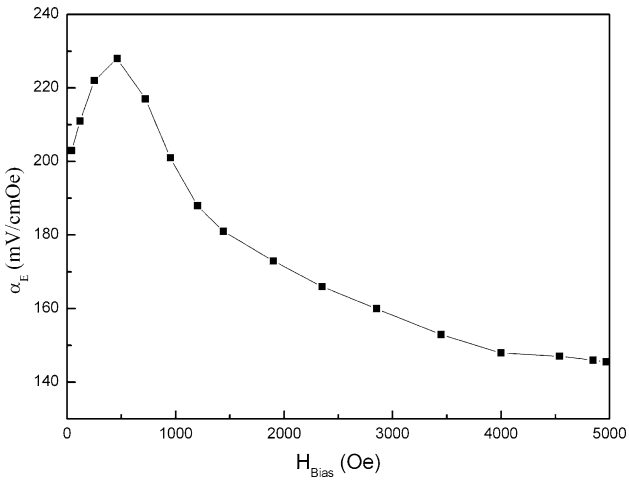

Fig. 7 Variations of α_E with H_{Bias} for the $P_2C_4P_2C_4P_2$ composite film

composite films is greater than that of some other corresponding results of the CFO–PZT composite film in the literature [20] (about 35 mV/cm Oe). With the further increase of H_{bias}, the α_E decreases gradually to 145 mV/cm Oe when H_{bias} is 5000 Oe.

In the magnetostrictive–ferroelectric composite system (e.g., the CFO–PZT composite), ME coupling mainly arises from the magnetic–mechanical–electric transform through the stress-mediated transfer in the interface. The dynamic magnetoelastic coupling caused by the magnetostriction of the CFO phase, which is due to the domain-wall motion and the rotation of the magnetic domain, is involved in the ME effect. Therefore, the low coercivity and high magnetostriction are advantageous for a strong ME effect [26]. In CFO bulk materials, the rotation of magnetic domain is greatly limited as CFO materials are difficult to be magnetized with a greater coercivity more than 2000 Oe [27]. However, in the composite film, the H_c of the CFO films is lower than that of CFO bulk materials, the composite film exhibits an easy-magnetization characteristic, which is advantageous for the rotation of magnetic domain. This results in a larger magnetostriction under a very low magnetic field, consequently leads to a strong ME coupling by interface coupling.

As for the H_{bias} dependence of α_E, it essentially tracks the H_{bias} dependence of the piezomagnetic coupling coefficient $q = d\lambda/dH_{bias}$ [26, 28] (where λ is the magnetostriction). For the CFO phase, once the magnetostriction attains the saturation value, the q decreases and the piezomagnetic coupling becomes gradually weak, resulting in the decrease of the ME effect.

The highest α_E of the composite film is obtained when H_{bias} is near 460 Oe. This indicates that the magnetostriction of the CFO phase has reached a saturation value and produced a constant electric field in the piezoelectric phase. Then the dE/dH decreases with the further increase of

H_{bias}. This also shows that magnetic saturation occurs at low stimulation and the composite film is best suitable for being used at relatively weak H_{bias}. The behavior of the magnetic field dependence of ME voltage coefficient is similar to that for the magnetostrictive behavior [29].

Conclusion

In summary, the ME composite film ($P_2C_4P_2C_4P_2$) has been successfully prepared by using a simple sol–gel method and spin-coating technique. XRD results show that PZT and CFO phases exist besides phases in substrate after calcined at 700 °C, and no obvious impurity phases can be detected. The composite film has well-defined layer boundaries between CFO and PZT films. The composite film exhibits both good magnetic and electric properties, as well as ME effect. The magnetic parameters such as M_s and H_c were also measured. The presence of ferroelectric phase affects the values of M_s and M_r. Ferroelectric hysteresis loop reveals that saturated polarization and remanent polarization are lower than those of the pure PZT films due to the dilute influence of CFO phase on the composite film. The ME sensitivity of the composite film illustrates the strong dependence on the H_{bias}. With increasing the magnetic field H_{bias}, the α_E increases rapidly to reach its highest value near 460 Oe and then rapidly decreases. In particular, the composite film exhibits a very great ME effect, which makes the composite film attractive for technological applications as devices.

Acknowledgements The authors wish to acknowledge the financial support of this research from Specialized Research Fund for the Doctoral Program of Higher Education of China (200803591037) and the Scientific Research Fund of Hefei University of Technology for Doctor Degree (GDBJ2008-008).

References

1. Spaldin NA, Fiebig M (2005) Science 309:391
2. Dho XQJ, Kim H, MacManus-Driscoll JL, Blamire MG (2006) Adv Mater 18:1445
3. Nan CW (1994) Phys Rev B 50:6082
4. Yan L, Yang YD, Wang ZG, Xing ZP, Li JF, Viehland D (2009) J Mater Sci 44:5080. doi:10.1007/s10853-009-3679-1
5. Deng CY, Zhang Y, Ma J, Lin YH, Nan CW (2008) Acta Mater 56:405
6. Wang J et al (2003) Science 299:1719
7. Zheng H et al (2004) Science 303:661
8. Levin I, Li JH, Slutsker J, Roytburd AL (2006) Adv Mater 18:2044
9. Zhou JP, He HC, Shi Z, Nan CW (2006) Appl Phys Lett 88:013111
10. He HC, Wang J, Zhou JP, Nan CW (2007) Adv Funct Mater 17:1333
11. He HC, Zhou JP, Wang J, Nan CW (2006) Appl Phys Lett 89:052904
12. Wang Y, Nan CW (2006) Appl Phys Lett 89:052903
13. Zhan Q et al (2006) Appl Phys Lett 89:172902
14. Zhang Y, Deng CY, Ma J, Lin YH, Nan CW (2008) Appl Phys Lett 92:062911
15. Xie SH, Li JY, Qiao Y, Liu YY, Lan LN, Zhou YC, Tan ST (2008) Appl Phys Lett 93:222904
16. Fina I, Dixa N, Fàbrega L, Sánchez F, Fontcuberta J (2010) Thin Solid Films 518:4634
17. Delgado E, Ostos C, Martínez-Sarrión ML, Mestres L, Lederman D, Prieto P (2009) Mater Chem Phys 113:702–706
18. Wan JG, Wang XW, Wu YJ, Zeng M, Wang Y, Jiang H, Zhou WQ, Wang GH, Liu JM (2005) Appl Phys Lett 86:122501
19. Liu M, Li X, Lou J, Zheng SJ, Du K, Sun NX (2007) J Appl Phys 102:083911
20. Wan JG, Zhang H, Wang XW, Pan DY, Liu JM, Wang GH (2006) Appl Phys Lett 89:122914
21. Patil DR, Chougule BK (2009) J Mater Sci 20:398. doi:10.1007/s10854-008-9742-x
22. Chen W, Chen XF, Wang ZH, Zhu W, Tan OK (2009) J Mater Sci 44:4939. doi:10.1007/s10853-009-3754-7
23. Haertling GH (1999) J Am Ceram Soc 82:797
24. Boomgaard JVD, Born RAJ (1978) J Mater Sci 13:1538. doi:10.1007/BF00553210
25. Boomgaard JVD, Run AMJGV, Suchetelene JV (1976) Ferroelectrics 10:295
26. Srinivasan G, Rasmussen ET, Gallegos J, Srinivasan R, Bokhan YI, Laletin VM (2001) Phys Rev B 64:214408
27. Sathaye SD, Patil KR, Kulkarni SD, Bakre PP, Pradhan SD, Sarwade BD, Shintre SN (2003) J Mater Sci 38:29. doi:10.1023/A:1021101529855
28. Zeng M, Wan JG, Wang Y, Yu H, Liu JM, Jiang XP, Nan CW (2004) J Appl Phys 95:8069
29. Mazumder S, Bhattacharyya GS (2004) Ceram Int 30:389